RIGOROUS 3D EM SIMULATION AND AN EFFICIENT APPROXIMATE MODEL OF MMIC OVERLAY CAPACITORS WITH MULTIPLE FEEDPOINTS

M. Engels and R.H. Jansen

Duisburg University, Dept. of Electrical Engineering,
FB9/HHFT, Bismarckstr. 81, W-4100 Duisburg 1, Germany

ABSTRACT

A systematic 3D electromagnetic analysis of MIM-capacitors with up to 4 feedstrips has been performed to investigate the electrical effects of feed widths and positions. Based on this, an efficient approximate CAD model of MIM-capacitor N-ports has been developed which is an extension and generalization of a recently published two-port model.

INTRODUCTION

The MIM-capacitor, also called overlay capacitor, is a standard component in MMICs mainly used for DC blocking and as a matching element up to high mm-wave frequencies. At relatively low frequencies, it can be well modelled as a simple lumped parallel plate capacitance appropriately corrected by a small stray field term /1/, /2/, /3/. With the growing sophistication of CAD tools for MMIC design, more elaborate models have been developed using essentially a lumped capacitance in combination with a transmission line that represents the substrate effects, see for example /4/, /5/. Further improved models are based on a 2D distributed approach treating the MIM capacitor structure as a broadside coupled strip transmission line configuration /6/, /7/, /8/. However, none of the mentioned models is capable of calculating capacitors taking into account the electrical effects of off-center feedstrips. Such effects were only recently considered by Giannini /9/ using a specific modification of the so-called "Planar circuit model" /10/ including the ground and feedstrip effects for two-port MIM-capacitors. The model presented here is an extension and generalization of this and is applicable to MIM-capacitors of rectangular shape with an arbitrary number of feedstrips connected at arbitrary sides of the structure. Systematic investigations have been made for capacitors with up to 4 feedpoints, one at each side. In order to achieve this level of generalization, effective feeding parameter descriptions have been developed for the various possible feedpoint configurations which take into account the feed related stray fields. It is clearly shown that the feeding configuration has to be considered for accurate MIM-capacitor modelling at high microwave frequencies. The general model presented here /11/ is suitable for interactive CAD. It has been verified systematically by comparison to rigorous results generated by means of a commercial full-wave 3D electromagnetic simulator /8/, /12/, /13/, studying the electrical effects of overlay capacitors at very high frequencies as a function of various common feed configurations. This approach has been chosen, since availability of broadband measured MIM-capacitor data is very limited and essentially restricted to two-port S-parameters and the in-line configuration.

FEED RELATED PARASITICS

A few typical MIM capacitor configurations investigated are shown in Fig. 1, all of these having the same overlay plate geometry but using different feed strips and feed positions.

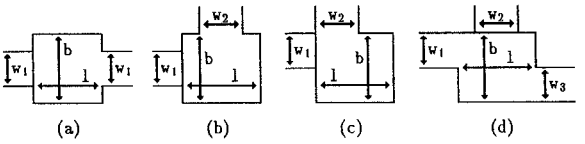

Fig. 1 Some MIM-capacitor configurations commonly used in MMICs

The in-line feed situation of Fig. 1(a) is the one represented best by the conventional modelling approaches /1/-/7/. Here, the reflection coefficient magnitude increases at higher frequencies in contrast to that of an ideal capacitor due to the parasitic capacitance of the lower capacitor plate to ground. Parasitic effects are more pronounced for configurations like 1(b) and 1(c), in particular, so that conventional models have poor accuracy in these cases. This is shown in Fig. 2.

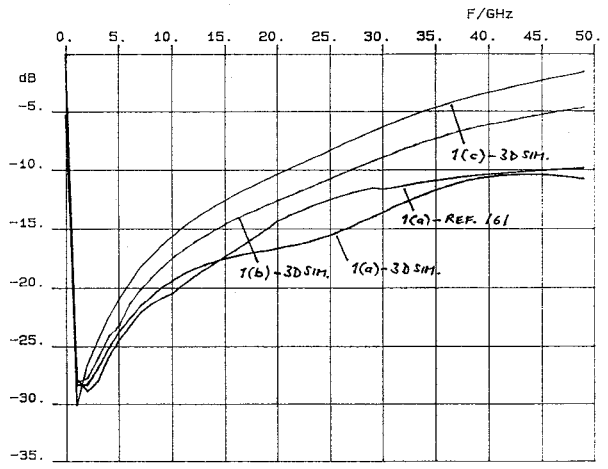

Fig. 2 Comparison of S-parameters computed for the cases of Fig. 1(a)...(c), SiN dielectric 0.1 m on GaAs substrate, dimensions l=b=288m, $W_1=W_2=144$m feed strips.

An example of a 3-port capacitor with generalized feed configuration is given in Fig. 1(d). For such configurations, truly layout-oriented and distributed models have not yet been reported to date. The rigorous electromagnetic computation of these cases shows, that the magnitudes of the port reflection and transmission coefficients split at higher frequencies in a significant way, which is an effect not predicted by the commonly used models with the feedstrip connection simply represented by a multiple node. The reason for this observed splitting is a distributed junction effect and a nonsymmetrical excitation of the component.

At high microwave frequencies the capacitor plates appear essentially short-circuited, so that the capacitor behaves similar to a respective junction with only one metallization level. This is approximately true at least for the S-parameter magnitudes, while the situation is more complicated for the phase angles. For example, the in-line capacitor configuration with widths of feedlines and plates equal behaves very much like a short length of thru-line at high frequencies. This is applied frequently for DC blocking. The in-line configuration with unequal widths of feed strips and plates, see Fig. 1(a), behaves much like a thru-line with a step in width. Consequently, the port reflection coefficients increase again at high frequencies in contrast to those of an ideal series capacitor.

Another type of parasitic effect is associated with MIM capacitors, if the feed strips are arranged at a geometrical angle of 90 degrees. In this case, there is a noticeable deviation from ideal electrical capacitor behaviour even if feed strips and plates have equal widths. Our investigations have shown that the reason for this is mainly the different spatial distribution of the stray field to ground of the lower capacitor plate as compared to the symmetric case of Fig. 1(a). The stray capacitance to ground is considerably larger in the configuration of Fig. 1 (b). In addition, there is the effect of RF current density crowding for such bend-type structures.

The parasitic effects in multiport capacitors like that in Fig. 1(d) are more complex and obviously caused by a superposition of the outlined fundamental effects. As a general rule of thumb, multiport capacitors have much in common electrically with multiport junctions consisting of just one conductor level and having the same shape, once the frequency is high enough to essentially produce an RF short circuit in the center of the structure.

N-PORT MIM CAPACITOR MODEL

The general MIM-capacitor configuration modelled in this contribution is comprised by two loosely coupled field regions, region (I) between the capacitor plates (with some air stray field included) and region (II) between the lower plate and the ground plane (again with some stray field in the air included). Following the planar circuit approach, each of these two open regions is separately replaced here by a respective closed one that is laterally bounded by magnetic walls. The respective geometric dimensions and dielectric constants are replaced by effective ones, as indicated in Fig. 3(a) and 3(b). Taking feedstrips into account, for each of the regions I and II, a floor-plan as shown in Fig. 3(c) results.

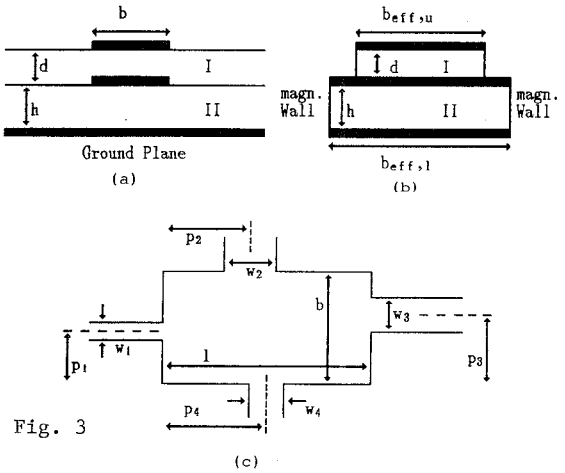

Fig. 3

For convenience, the subscripts addressing the individual region, and indicating that the parameters are effective ones, have been omitted in Fig. 3(c). Accordingly, the impedance matrix for each of the two closed magnetic wall approximations I and II can be written as /10/:

$$Z_{ik} = j\omega\mu h \sum_{n=0}^{\infty}\sum_{m=0}^{\infty} \frac{P_{mni}\, P_{mnk}}{K_{mn}^2 - \omega^2\mu\epsilon_{mn}} \qquad \text{(Eq. 1a)}$$

$$K_{mn}^2 = \left(\frac{m\pi}{l}\right)^2 + \left(\frac{n\pi}{b}\right)^2 \qquad \text{(Eq. 1b)}$$

$$P_{mnj} = \frac{1}{w_{eff}} \int_{s_j} E_{mnz}\, ds\,. \qquad \text{(Eq. 1c)}$$

In order to obtain our generalized N-port MIM-capacitor model, the two separate representations of region I and II, respectively, have to be interconnected appropriately. This interconnection is made in such a way that port voltages related to the upper level capacitor plate are suitably divided into two portions, one portion associated with region I, the other one related to field region II. Voltages related to feed strips on the lower plate metal level are associated with region II only. This is illustrated below in Fig. 4 schematically with voltage vectors (V_I), (V_{II}) and represented mathematically by Eq. 2.

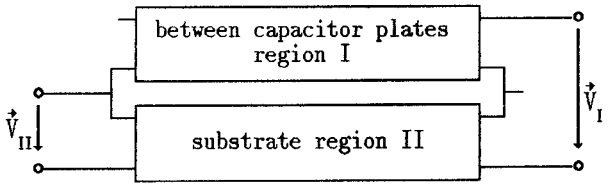

Fig. 4 Illustration of the interconnection of the field regions I and II

$$\overleftrightarrow{Z}_{cap} = \overleftrightarrow{Z}_l + \overleftrightarrow{\delta}\cdot\overleftrightarrow{Z}_u\cdot\overleftrightarrow{\delta}\,. \qquad \text{(Eq. 2)}$$

$$\overleftrightarrow{\delta} = \begin{bmatrix} \delta_1 & 0 & \cdots & 0 \\ 0 & \delta_2 & \cdots & 0 \\ \vdots & & \ddots & \vdots \\ 0 & 0 & \cdots & \delta_n \end{bmatrix} \qquad \delta_i = \begin{cases} 1 & \text{; port i on upper capacitor plate} \\ 0 & \text{; port i on lower capacitor plate} \end{cases}$$

(Eq. 2)

To obtain good agreement with rigorous results obtained by 3D electromagnetic analysis, it is quite important to describe the effective dimensions associated with regions I, II correctly, particularly those of the substrate region and those associated with specific feed situations. In calculating effective dimensions for the developed multiport model, the assumption is made that stray fields for the individual rectangular conductor shapes (feed strips and capacitor plates) can be represented in the same way as is usual for strip transmission lines. This implies, that the effective geometry of the substrate region II results by removing the top metallization and then computing the effective dielectric constant and the effective field volume of this region. Where a feed strip is attached, a respective portion of the volume is removed again. Composite substrate effective parameters are taken from multidielectric microstrip analysis like the one integrated in the CAD package /8/. Effective dimensions are also taken into account for region I though simple parallel plate formulae may be sufficient for thin capacitor dielectrics and for large capacitor areas. However, for the purpose of general applicability, region I effective parameters have been derived too under inclusion of stray fields making use of Wheeler's formulae /14/. Therefore, they are valid with good accuracy even for small area plates and relatively large plate spacings. The basic procudure how effective dimensions are computed in the N-port capacitor model developed is illustrated in Fig. 5.

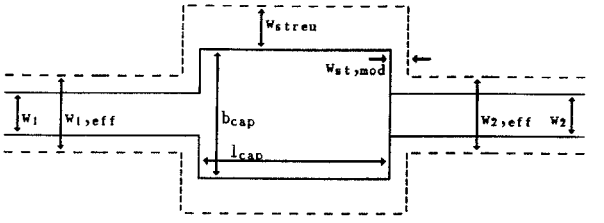

Fig. 5 Illustration of effective capacitor dimensions used for stray field evaluation

Specifically, the effective stray field width at a capacitor side without feedstrip is calculated as

$$w_{st} = \frac{l_{eff} - l_{cap}}{2} \quad \text{or} \quad w_{st} = \frac{b_{eff} - b_{cap}}{2}\,.$$

With feedstrips connected, a modified effective width applies to the respective capacitor side following the relation

$$w_{st,mod} = w_{st} \cdot \frac{b_{eff} - w_{i,eff}}{2\cdot b_{eff}}\,,$$

or

$$w_{st,mod} = w_{st} \cdot \frac{l_{eff} - w_{i,eff}}{2\cdot l_{eff}}\,.$$

In this expression, the factor of 2 occurring in the denominator is an empirical correction factor that has been found to provide good agreement with rigorous numerical 3D EM simulations. Further modification of the effective geometrical dimensions becomes necessary, if small size capacitors are analyzed. In that case, stray fields of the feed lines may overlap which requires an additional correction term.

RESULTS AND DISCUSSION

As a first example demonstrating the new generalized capacitor model, Fig. 6a shows the reflection coefficients (magnitudes) at all three ports of the configuration of Fig. 1(d) in comparison to the rigorous 3D electromagnetic analysis. The substrate and dielectric parameters are again those of Fig. 2. Since the considered capacitor is relatively large and the analysis of Fig. 6a was made with frequency steps of 1 GHz, a sharp transition is visible at f=1GHz (curves are piecewise linear) which is of course smooth for finer discretization. Even though the capacitor is large, the developed model is very accurate up to about 20 GHz and gives reasonable accuracy over the full range up to 50 GHz. This is even more obvious from Fig. 6b where the transmission coefficients of the same 3-port capacitor are given. The transmission coefficients of the developed approximate model agree well with the 3D EM data over the full frequency range up to 50 GHz considered. Besides this, the model has a very high computation speed suitable for interactive CAD. The new model includes feeding effects which can be crucial at higher frequencies and thus represents an improvement of the state-of-the-art of modelling for an important class of passive MMIC components.

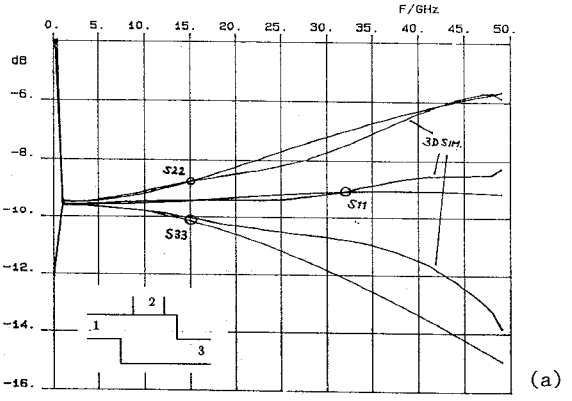

(a)

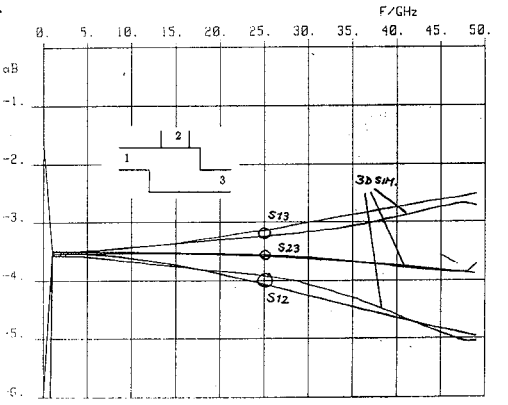

(b)

Fig. 6 Reflection magnitudes (a), and transmission magnitudes (b) developed model versus rigorous electromagnetic analysis for a 3-port MIM capacitor

REFERENCES

/1/ D.A. Daly et al., IEEE Trans., vol. MTT-15, 1967, 713-721

/2/ I. Wolff et al., Proc. IEE Colloquium on CAD of microwave circuits, IEE Publ. 1985/99, London, Nov. 1985, Paper 1/1-3

/3/ E. Pettenpaul et al., IEEE Trans., vol. MTT-36, 1988, 294-304

/4/ V.K. Sadhir and I.J. Bahl, Microwave and Optical Tech. Letters, vol. 4, No. 6, 1991, 219-222

/5/ W. Lam et al., IEEE MTT-S Symp. Digest, New York, 1988, 477-480

/6/ R.H. Jansen, Alta Frequenza (Italy), vol. LVIII, No. 5-6, 1989, 551-558

/7/ J.P. Mondal, IEEE Trans., vol. MTT-35, 1987, 403-408

/8/ LINMIC+/N Computer Program and Users Manual, Versions 2.2/90...3.0/92, Jansen Microwave, Ratingen, Germany

/9/ F. Giannini et al., Proc. GaAs'92 European GaAs Applications Symposium, Noordwijk, The Netherlands, April 1992, Poster Session, Paper No. 5

/10/ G. D'Inzeo et al., IEEE Trans., vol. MTT-26, 1978, 462-471

/11/ M. Engels, MS EE thesis (in German), Duisburg University, EE Dept. FB9/HHFT, Oct. 1992

/12/ R.H. Jansen, Microwave Eng. Europe Journal, April 1991, 21-24

/13/ R.H. Jansen and J. Sauer, IEEE MTT-S Symp. Digest, Boston, 1991, 1087-1091

/14/ H.A. Wheeler, IEEE Trans., vol. MTT-13, 1965, 178-185